Global Change Biology

Global Change Biology (2010) **16**, 657–670, doi: 10.1111/j.1365-2486.2009.01991.x

Assimilation exceeds respiration sensitivity to drought: A FLUXNET synthesis

CHRISTOPHER R. SCHWALM*, CHRISTOPHER A. WILLIAMS*, KEVIN SCHAEFER†, ALMUT ARNETH‡, DAMIEN BONAL§, NINA BUCHMANN¶, JIQUAN CHEN‖, BEVERLY E. LAW**, ANDERS LINDROTH‡, SEBASTIAAN LUYSSAERT††, MARKUS REICHSTEIN‡‡ and ANDREW D. RICHARDSON§§

*Graduate School of Geography, Clark University, Worcester, MA 01610, USA, †Cooperative Institute for Research in Environmental Sciences, University of Colorado at Boulder, Boulder, CO 80309, USA, ‡Department of Physical Geography and Ecosystems Analysis, Lund University, SE-22362 Lund, Sweden, §INRA, UMR Ecologie des Forêts de Guyane, BP 709, 97387 Kourou Cedex, French Guiana, ¶Institute of Plant Sciences, ETH Zürich, CH-8092 Zürich, Switzerland, ‖Department of Environmental Sciences, University of Toledo, Toledo, OH 43606, USA, **College of Forestry, Oregon State University, Corvallis, OR 97331, USA, ††Department of Biology, University of Antwerp, 2610 Wilrijk, Belgium, ‡‡Biogeochemical-Model-Data Integration Group, Max-Planck Institute for Biogeochemistry, 07701 Jena, Germany, §§Complex Systems Research Center, University of New Hampshire, Durham NH 03824, USA

Abstract

The intensification of the hydrological cycle, with an observed and modeled increase in drought incidence and severity, underscores the need to quantify drought effects on carbon cycling and the terrestrial sink. FLUXNET, a global network of eddy covariance towers, provides dense data streams of meteorological data, and through flux partitioning and gap filling algorithms, estimates of net ecosystem productivity (F_{NEP}), gross ecosystem productivity (P), and ecosystem respiration (R). We analyzed the functional relationship of these three carbon fluxes relative to evaporative fraction (EF), an index of drought and site water status, using monthly data records from 238 micrometeorological tower sites distributed globally across 11 biomes. The analysis was based on relative anomalies of both EF and carbon fluxes and focused on drought episodes by biome and climatic season. Globally P was $\approx$ 50% more sensitive to a drought event than R. Network-wide drought-induced decreases in carbon flux averaged -16.6 and $-9.3\,g\,C\,m^{-2}\,month^{-1}$ for P and R, i.e., drought events induced a net decline in the terrestrial sink. However, in evergreen forests and wetlands drought was coincident with an increase in P or R during parts of the growing season. The most robust relationships between carbon flux and EF occurred during climatic spring for F_{NEP} and in climatic summer for P and R. Upscaling flux sensitivities to a global map showed that spatial patterns for all three carbon fluxes were linked to the distribution of croplands. Agricultural areas exhibited the highest sensitivity whereas the tropical region had minimal sensitivity to drought. Combining gridded flux sensitivities with their uncertainties and the spatial grid of FLUXNET revealed that a more robust quantification of carbon flux response to drought requires additional towers in all biomes of Africa and Asia as well as in the cropland, shrubland, savannah, and wetland biomes globally.

Keywords: biome, carbon cycling, drought, eddy covariance, evaporative fraction, FLUXNET, synthesis

Received 11 February 2009; revised version received 22 May 2009 and accepted 23 May 2009

Introduction

The exchange of CO_2 between the land surface and the atmosphere is an important pathway in the global carbon cycle. From 2000 to 2006 the net carbon sink along this pathway averaged $2.8\,Pg\,C\,yr^{-1}$ or 37% of global fossil fuel emissions (Canadell *et al.*, 2007). This average value masks seasonal and interannual variability in CO_2 metabolism. At scales of 0.1–1 km^2 this variability has been linked to ecosystem state variables (Schwarz *et al.*, 2004; Barr *et al.*, 2007; Houghton, 2007),

Correspondence: Christopher R. Schwalm, tel. +1 508 793 7336, fax +1 508 793 8881, e-mail: cschwalm@clarku.edu

© 2009 Blackwell Publishing Ltd

disturbance (Lindroth *et al*., 2009), site history (Law *et al*., 2002), and year-to-year variability in weather (Houghton, 2000; Richardson *et al*., 2007; Baldocchi, 2008). Superimposed on this variability is a linear warming trend (Trenberth *et al*., 2007) with increased weather variability and concomitant increases in extreme weather events and climate anomalies.

As part of this global trend in climate, the incidence and severity of drought has increased. Dai *et al*. (2004b) showed that the global total of very dry land areas (Palmer Drought Severity Index < -3.0) has increased from 12% to 30% since 1972. Regional to continental scale increases in drought incidence have been documented in Canada (Shabbar & Skinner, 2004), northern Eurasia (Groisman *et al*., 2007), and parts of China (Zou *et al*., 2005). Recent large-scale and severe droughts have occurred in Europe in 2003 (Ciais *et al*., 2005), western North America from 1999 to 2004 (Cook *et al*., 2004), the Sahel region of Africa from the 1960s to present (Dai *et al*., 2004a), Amazonia in 2005 (Bonal *et al*., 2008; Marengo *et al*., 2008), and Australia in 2002–2003 (Nicholls, 2004). Although the increase in drought is variable across time and space and is confounded by operationally inconsistent definitions and indices of drought (Heim, 2002) and spatiotemporal limitations of baseline data (Huntington, 2006), the overall trend supports both an intensification of the hydrological cycle and more severe drought episodes (Huntington, 2006; Trenberth *et al*., 2007).

Despite the known link between interannual variability in weather and terrestrial carbon cycling and the documented increase in drought, i.e., extreme weather incidence and severity, the response of carbon fluxes to extreme hydrological conditions is poorly constrained. Studies based on eddy covariance (EC) measurements, which provide estimates of net ecosystem productivity (F_{NEP} where values >0 indicate a net drawdown of atmospheric CO_2), gross ecosystem productivity (P), and total ecosystem respiration (R) show that flux responses to drought events are uncertain in both magnitude and direction. Kljun *et al*. (2007) observed, during a drought in western boreal Canada, an increase in both F_{NEP} (1.5 times predrought value) and P in an aspen forest and largely no effect in two boreal coniferous systems. As the drought entered its second year all three fluxes decreased at the aspen site; postdrought yearly flux integrals were also less than predrought values. During the 2003 drought in Europe Reichstein *et al*. (2007a) found that nine of the 14 sites affected had negative flux anomalies relative to the predrought condition. Response magnitude (predrought–postdrought flux value $g\,C\,m^{-2}\,month^{-1}$) ranged from -117 to $+29$ for P; -89 to $+21$ for R and -73 to $+30$ for F_{NEP}. Pereira *et al*. (2007) examined three Mediterranean sites across 4 hydrological years, two of which were dry, and found diverging patterns: All three carbon fluxes in an *Eucalyptus* plantation decreased during the drought years; with the absolute largest decrease occurring in the second drought year. At an evergreen oak-dominated site F_{NEP} increased in each dry year. CO_2 metabolism at the Mediterranean grassland site decreased during drought and switched from a sink to source (Pereira *et al*., 2007). Finally, in a neotropical rainforest in French Guiana, South America F_{NEP} increased during a severe drought episode in 2005 due to a decrease in R and a conservative response in P (Bonal *et al*., 2008). This ambiguity in flux response is confounded by antecedent effects (e.g. water storage in the soil column), the rarity of droughts and resulting low sampling intensity (Baldocchi, 2008), sampling of intra- vs. interannual drought episodes, stand age (Law *et al*., 2001), plant functional type (PFT; Granier *et al*., 2007), and operational definitions of drought (Heim, 2002).

In this analysis, we evaluate the functional response of carbon fluxes to drought using a drought index and data from FLUXNET; a global network of 13 regional flux tower networks that coordinates the processing, warehousing, and analysis of observations on terrestrial carbon cycling from micrometeorological tower sites (Baldocchi, 2008). Specifically, we are interested in (i) quantifying both magnitude and direction of flux response to drought, (ii) determining to what degree functional coherence in flux response to drought exists, and (iii) extending point-based functional understanding to scales that are useful in quantifying continental carbon exchanges from a sparse observation network.

Methods

Carbon fluxes and drought metric

Carbon fluxes were estimated using the EC method (Baldocchi *et al*., 2001) at FLUXNET site locations (Table 1; Fig. 1) included in the La Thuile and Asilomar FLUXNET Synthesis dataset (http://www.fluxdata.org/). Postprocessing of EC data followed standardized protocols CO_2 fluxes were corrected for storage, despiked, u^*–filtered, and gap-filled (Papale *et al*., 2006; Moffat *et al*., 2007). Each site measured F_{NEP} and provided estimates of P and R through flux partitioning algorithms (Papale & Valentini, 2003; Reichstein *et al*., 2005). Data were aggregated to monthly flux integrals ($n = 5173$ months) and used only if more than 90% of the half-hourly values in a given month were either direct measurements or gap-filled with high confidence.

Evaporative fraction (EF) was used as an index of drought (San Miguel-Ayanz *et al*., 2000; Heim, 2002) and

Table 1 Biome classifications (Belward & Loveland, 1996) sampled at FLUXNET sites with number of sites (n_{site}) and monthly observations (n_{month}) used in flux sensitivity estimation

Biome code	Description	n_{site}	n_{month}
CRO	Croplands: Lands covered with temporary crops followed by harvest and a bare soil period (e.g., single and multiple cropping systems)	29	415
CSH	Closed Shrublands: Lands with woody vegetation less than 2 m tall and with shrub canopy cover >60%. The shrub foliage can be either evergreen or deciduous	4	115
DBF	Deciduous Broadleaf Forests: Lands dominated by woody vegetation with a percent cover >60% and height exceeding 2 m. Consists of broadleaf tree communities with an annual cycle of leaf-on and leaf-off periods	29	832
EBF	Evergreen Broadleaf Forests: Lands dominated by woody vegetation with a percent cover >60% and height exceeding 2 m. Almost all trees and shrubs remain green year round. Canopy is never without green foliage	18	486
ENF	Evergreen Needleleaf Forests: Lands dominated by woody vegetation with a percent cover >60% and height exceeding 2 m. Almost all trees remain green all year. Canopy is never without green foliage	67	1745
GRA	Grasslands: Lands with herbaceous types of cover. Tree and shrub cover is <10%. Permanent wetlands lands with a permanent mixture of water and herbaceous or woody vegetation. The vegetation can be present in either salt, brackish, or fresh water	45	725
MF	Mixed Forests: Lands dominated by trees with a percent cover >60% and height exceeding 2 m. Consists of tree communities with interspersed mixtures or mosaics of the other forest types. None of the forest types exceeds 60% of landscape	14	295
OSH	Open Shrublands: Lands with woody vegetation <2 m tall and with shrub canopy cover between 10% and 60%. The shrub foliage can be either evergreen or deciduous	12	162
SAV	Savannas: Lands with herbaceous and other understory systems, and with forest canopy cover between 10% and 30%. The forest cover height exceeds 2 m	3	54
WET	Permanent Wetlands: Lands with a permanent mosaic of water and herbaceous or woody vegetation. The vegetation can be present in either salt, brackish, or fresh water	9	110
WSA	Woody Savannas: Lands with herbaceous and other understory systems and with forest canopy cover between 30% and 60%. The forest cover height exceeds 2 m	8	234

Includes only those sites ($n_{site} = 238$) with quality controlled flux data.

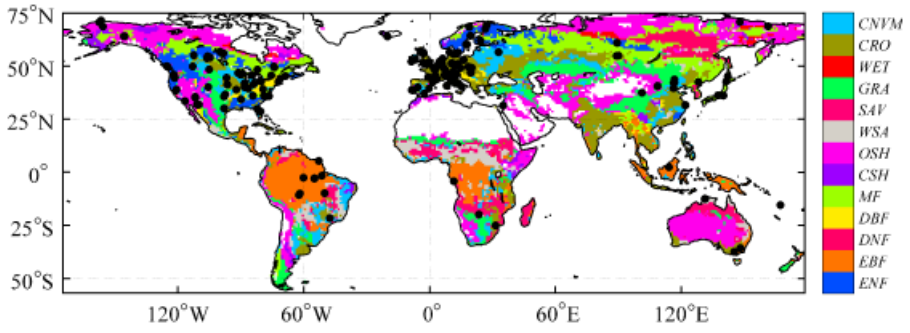

Fig. 1 Global 1° grid of dominant terrestrial biome and flux tower location (solid black circle). Only flux towers used in this data synthesis shown ($n = 238$). Biome classification of tower footprint may not match dominant biome classification at 1° resolution. Nonvegetated biomes shown in white.

is a function of tower-based heat fluxes given by

$$\mathrm{EF} = \frac{\lambda E}{\lambda E + H}, \quad (1)$$

where H (GJ m^{-2} month^{-1}) is sensible heat and λE (GJ m^{-2} month^{-1}) latent heat – both calculated using the same quality controls as the carbon fluxes. EF is related to the partitioning of available energy and therefore to energy balance closure at EC installations. Flux towers typically do not exhibit closure due to different levels of sensor error, unmeasured storage terms, mismatches in source area, and landscape heterogeneity (Baldocchi *et al.*, 2001; Wilson *et al.*, 2002; Foken, 2008; Shao *et al.*, 2008). However, EF can

be written as

$$\mathrm{EF} = \frac{1}{1 + H/\lambda E}\,. \quad (2)$$

We assume the errors in H and λE are of similar magnitude (Hollinger & Richardson, 2005; Richardson *et al*., 2006; Foken, 2008) and uncorrelated; this allows the lack of closure to cancel mathematically.

Relevance of EF to drought events

In terms of biophysical process EF is linked to precipitation, soil moisture, and temperature, especially in summer (Trenberth & Guillemot, 1996). As the quantity of near surface soil moisture declines, less available energy is used for vaporization, more is available for conduction and convection (Kurc & Small, 2004); H and temperature increase whereas EF decreases. The exact trajectory of EF is mediated by its initial value, rooting depth, soil water holding capacity (Mu *et al*., 2007), precipitation phase, and seasonality. In contrast, as $\mathrm{EF} \to 1$, most available energy is λE and water flows uninhibited through the soil–plant–atmosphere continuum reflecting sufficient plant available water due to adequate rainfall, subsurface flow, and root access to deep groundwater.

In addition EF is an index of water deficit. Under a steady-state surface energy balance (Brutsaert, 1982), equilibrium evaporation is

$$\lambda E_{eq} = (\lambda E + H)\frac{\Delta}{\Delta + \gamma}\,, \quad (3)$$

where $\Delta(\mathrm{Pa\,K^{-1}})$ is the rate of change of saturation specific humidity with air temperature and γ is the psychometric constant ($66\,\mathrm{Pa\,K^{-1}}$). Comparing Eqn (3) with Eqn (2) shows that

$$\mathrm{EF}\frac{\Delta + \gamma}{\Delta} = \frac{E}{E_{\mathrm{eq}}}\,. \quad (4)$$

EF then expresses, discounting a minor temperature adjustment, the ratio of actual (E) to equilibrium evapotranspiration (E_{eq}). Whether evaluated at climate timescales (years to decades) or meteorological timescales (minutes to months), this ratio is widely viewed as an index of water deficit ranging from 0 when fully dry to 1 when fully wet.

Finally, when viewed in conjunction with known drought episodes, EF, based on its linkages to biophysical process, tracked the decline in carbon flux (F_{NEP}, P, and R) anomalies for both the 1999–2003 drought in western North America (Cook *et al*., 2004; Kljun *et al*., 2007) and the 2003 drought in Europe (Reichstein *et al*., 2007a) (Fig. 2).

Analytical framework

Before estimating flux response to drought, each carbon flux and EF were deseasonalized and transformed into relative anomalies, i.e. normalized to have mean zero and unit variance by site and climatic season. Season was determined by calendar month and hemisphere, e.g. climatic winter consists of northern hemisphere data collected in December, January, and February and southern hemisphere data from June, July, and August. The use of climatic season focused the analysis on interannual rather than seasonal dynamics by removing the within-season mean across the full data record for a given site. Furthermore, normalization homogenized the range in EF (Fig. 3) and carbon fluxes thereby removing the spatial gradient in both (Lauenroth & Sala, 1992). This rescaling resulted in all sites having episodes of relative drought. Finally, monthly values with a mean air temperature $<0\,^{\circ}\mathrm{C}$ were removed from the analysis to exclude carbon flux response driven by cessation of photosynthesis, phenology, or cold temperature limitation.

The normalized data were then grouped by biome (Table 1), climatic season, and carbon flux. This created 132 data groups: 11 biomes $\times$ 4 climatic seasons $\times$ 3 carbon fluxes = 132 groups. Within a given group all months were treated as replicates and a least squares regression was performed with normalized EF as the explanatory variable and normalized carbon flux as the response. Preliminary testing of the functional form of normalized carbon flux regressed on normalized EF was based on the Akaike information criterion (AIC, Akaike, 1974; Hastie *et al*., 2003), a measure of goodness of fit for an estimated statistical model. We fit four models (linear, quadratic, cubic, logistic) to all 132 biome–climatic season–flux groups using the AIC with a second order correction for sample sizes (McQuarrie & Tsai, 1998). These models accommodate linear, arbitrarily curved, sigmoidal, and parabolic response surfaces. Across all groups the simple linear regression model had the lowest AIC value, i.e. was the model most consistent with the underlying structure of the data (Akaike, 1974; Hastie *et al*., 2003), and was retained throughout. The slope of this simple linear regression expressed a proportionality constant in normalized space or a relative sensitivity, i.e. quantified normalized carbon flux response in σ units (units of standard deviation) relative to unit σ change in normalized EF. However, the slope has an implicit denominator of $+1$, which indicated relative wetness. To recast the regression slope to express relative sensitivity in carbon flux to relative drought (hereafter: $\mathrm{d}F_{\mathrm{norm}}$) the sign convention was switched, i.e. numerator and denominator were multiplied by -1. Furthermore, we transformed

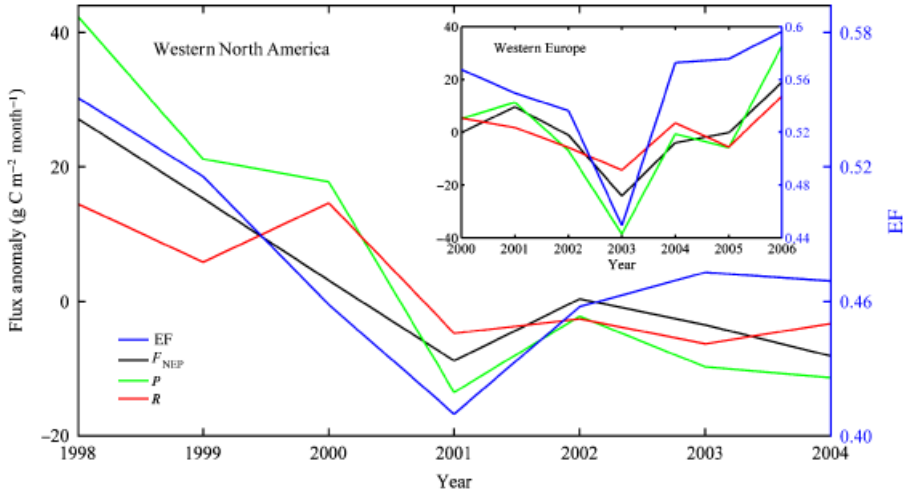

Fig. 2 Time series of evaporative fraction (EF) (dimensionless, blue line) and JJA flux anomalies (g C m^{-2} month^{-1}) for three carbon flux terms, F_{NEP} (black), P (green), and R (red), during two drought episodes. Flux anomalies calculated relative to labeled years only. In western North American (41 sites, eight biomes, main panel) drought severity and spatial extent increased starting 1999 and persisted through 2003. In western Europe (17 sites, seven biomes, inset) drought was shorter duration, more acute, and centered on summer 2003. In both instances EF was in phase to changes in drought-induced carbon flux anomalies.

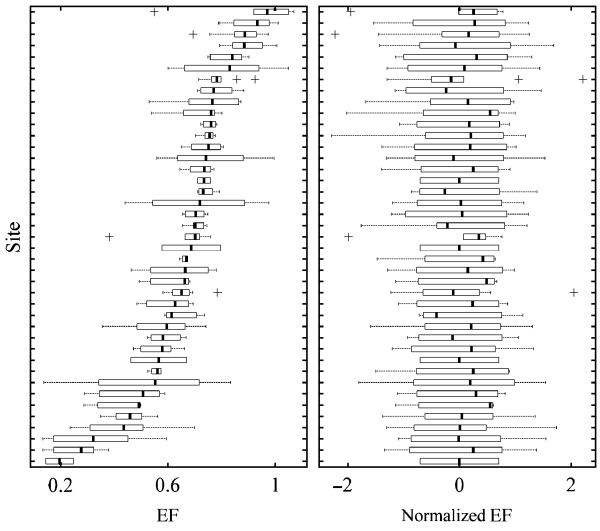

Fig. 3 Box plots of unnormalized evaporative fraction (EF) (dimensionless, left panel) and normalized EF (right panel) for GRA in climatic summer. Panels show interquartile range (box), median (solid black line), range (whiskers), and outliers (cross; values more than 1.5 × interquartile range from the median). Sites sorted by unnormalized median in both panels. Note that all means in the normalized EF panel are zero by definition. Data support for unnormalized EF was a function of site: EF followed a spatial gradient and only few sites showed drought-like conditions (low EF). Normalized EF lacked this trend, i.e. all sites shared an overlapping range with negative values indicative of relative drought.

dF_{norm} ($\sigma_{flux}-1\sigma_{EF}^{-1}$) to flux sensitivity (g C m^{-2} month^{-1} $-1\sigma_{EF}^{-1}$). This transformation to flux sensitivity (hereafter: dF) was achieved using the pooled standard, σ_F. That is, for each group-wise linear regression of normalized carbon flux on normalized EF the standard deviation across all unnormalized carbon flux values in that group was used to estimate σ_F with units g C m^{-2} month^{-1} σ_{flux}^{-1}, i.e. $dF = dF_{norm}\sigma_F$.

The uncertainty in flux sensitivity was calculated by combining the uncertainty from its two components, dF_{norm} and σ_F, in quadrature (Taylor, 1996; Lo, 2005). Uncertainty for dF_{norm} was 1 SE (standard error) of the estimated regression slope. For σ_F uncertainty was defined as 1 SE derived from mean σ_F across 1000 bootstrap replicates (Efron & Tibshirani, 1998). Finally, as this analysis required 132 hypothesis tests, one for each data group, the false discovery rate, i.e. the rate (q) of false rejections out of all rejections (Benjamini & Hochberg, 1995; Ventura *et al.*, 2004), was used to control for multiple comparisons at $q = 0.05$.

Scaling from biome to global patterns

Global flux sensitivity maps were generated by upscaling flux sensitivities and subsequently averaging over all climatic seasons. Flux sensitivities by climatic season were spatially scaled using the International Geosphere–Biosphere Program biome classification (1° resolution; Loveland *et al.*, 2001). For each terrestrial grid cell an area-weighted sum of flux sensitivities using all within grid cell biomes was calculated. These spatially upscaled grid cell values were then averaged using weights based on monthly FPAR (fraction of photosynthetically active radiation) normals, an independent measure of the seasonal variability in vegetation cover, i.e. the weighting emphasizes periods of

greater biological activity. Monthly normals of FPAR were derived from the Global Inventory Monitoring and Modeling Study (1° resolution; Tucker *et al*., 2005). Only 11 of the 16 terrestrial biome classifications were observed (Table 1; Fig. 1). Three of the unobserved biomes (barren lands, snow and ice, and urban areas) lack vegetative cover and were assigned a sensitivity of zero. For the unobserved cropland/natural vegetation mosaic biome (CNVM) the average of croplands (CRO), grasslands (GRA), mixed forest (MF), and open shrublands (OSH) was used. Finally, for deciduous needleleaf forests (DNF), also unobserved, the average of evergreen needleleaf forest (ENF) and DBF was used.

Results

Global patterns between EF and carbon cycling

Overall, the relationship between carbon fluxes (F_{NEP}, P, or R) and normalized EF was not the same across biomes. Furthermore, the response magnitude of P was greater than the response magnitude of R to relative drought. This held globally, by climatic season (Fig. 4) and by biome ($P < 0.01$; Table 2). Global flux sensitivities for P, R, and F_{NEP}, respectively, were −0.22, −0.18, −0.09 for dF_{norm} and −16.6, −9.3, −5.8 g C m^{-2} month^{-1} $-1\sigma_{EF}^{-1}$ for dF. This highlighted a general linear trend of decreased carbon sequestration under relatively drier moisture regimes. In normalized space, EF ranged from -2.9σ to $+3.3\sigma$ (median range by biome was -2.0σ to $+2.2\sigma$ during the warm season and -1.6σ to $+2.0\sigma$ in climatic winter) indicating that episodes of extreme relative dryness, i.e. drought events, were observed at FLUXNET sites. The distribution of both dF_{norm} and dF was negatively skewed with seven positive values, i.e. in seven biome–climatic season–flux groups relative drought was coincident with a relative increase in carbon flux. Sensitivities ranged from +0.58 to −0.86 and +14.8 to −126.4 g C m^{-2} month^{-1} $-1\sigma_{EF}^{-1}$ for dF_{norm} and dF, respectively (Table 2).

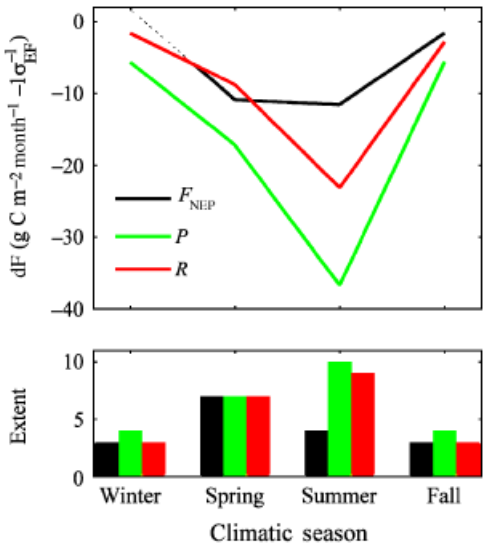

Fig. 4 Mean flux sensitivity (dF in g C m^{-2} month^{-1} $-1\sigma_{EF}^{-1}$) to relative drought across all biomes ($n = 11$) by climatic season (top panel) and extent, number of biomes with nonzero flux sensitivity (lower panel). F_{NEP} (black), P (green), and R (red).

Across biome and climatic season the seasonal peak, i.e. the largest value in magnitude, of network-wide flux sensitivity occurred during periods of peak biological activity (Fig. 4). This held for relative sensitivities of P and R, −0.44 and −0.42 in climatic summer, as well. In contrast, dF_{norm} for F_{NEP} peaked during climatic spring when, across all biomes, the terrestrial sink was largest. Furthermore, the overall ranking of carbon flux response to relative drought ($P < R < F_{NEP}$) held for all climatic seasons with the exception of flux sensitivities in climatic spring (Fig. 4). In this instance F_{NEP} was more sensitive to relative drought than P. The number of biomes where drought (normalized EF) acted as a control on carbon cycling (normalized carbon flux) varied by climatic season but was greatest during periods of peak biological activity (Fig. 4).

Uncertainties (Table 2) were variable across biome, climatic season, and flux and scaled with the magnitude of dF ($P < 0.05$; $r = 0.8$), i.e. the larger the flux sensitivity, the larger its associated uncertainty. Similarly, the largest uncertainties occurred during periods of peak biological activity, climatic spring and summer. Also, global flux uncertainty was largest for P and was 5.1, 2.8, and 2.0 g C m^{-2} month^{-1} $-1\sigma_{EF}^{-1}$ for P, R, and F_{NEP}, respectively. MF exhibited the largest average uncertainty by biome, followed by CRO: 10.5 and 9.9 g C m^{-2} month^{-1} $-1\sigma_{EF}^{-1}$, respectively. In contrast, the ENF biome had the smallest uncertainty ($= 3.6$ g C m^{-2} month^{-1} $-1\sigma_{EF}^{-1}$).

Spatial patterns in drought response

The largest carbon flux response occurred in three regions: the Midwest region of the United States and the prairie provinces of Canada, Eurasia extending eastward from France to Siberia, and eastern, particularly coastal, China (Fig. 5). In contrast, the tropical regions exhibited minimal sensitivity to relative drought. Mean monthly flux sensitivities, averaged across all grid cells, were −11.6, −7.6, −4.0 g C m^{-2} month^{-1} $-1\sigma_{EF}^{-1}$ for P, R, and F_{NEP}. Their corresponding uncertainties, 2.9, 1.9, 1.1 g C m^{-2} mon^{-1} $-1\sigma_{EF}^{-1}$ for P, R, and F_{NEP}, exhibited a similar spatial pattern (Fig. 6) and were proportional to grid cell flux sensitivity ($P < 0.0001$; $r \geq 0.9$).

Table 2 Summary of carbon flux $\sim EF$ relationships by biome and climatic season

		F_{NEP}			P			R		
Biome	Climatic season	dF_{norm}	dF	SE	dF_{norm}	dF	SE	dF_{norm}	dF	SE
CRO	Winter	–	–	–	–	–	–	–	–	–
	Spring	–	–	–	–	–	–	−0.23	−12.02	5.15
	Summer	−0.64	−80.60	9.72	−0.70	−126.43	13.92	−0.58	−43.61	5.78
	Fall	−0.30	−13.13	4.19	–	–	–	–	–	–
CSH	Winter	–	–	–	–	–	–	–	–	–
	Spring	−0.41	−12.13	5.27	–	–	–	–	–	–
	Summer	–	–	–	–	–	–	–	–	–
	Fall	–	–	–	–	–	–	–	–	–
DBF	Winter	–	–	–	−0.31	−3.58	1.55	−0.40	−8.08	2.71
	Spring	−0.70	−50.72	4.73	−0.78	−84.37	7.03	−0.70	−36.05	3.34
	Summer	−0.20	−12.35	3.62	−0.37	−33.14	5.16	−0.31	−19.89	3.71
	Fall	−0.21	−11.62	3.63	−0.31	−23.43	5.05	−0.35	−15.48	2.95
EBF	Winter	**0.30**	**10.71**	3.63	–	–	–	–	–	–
	Spring	−0.26	−10.97	3.74	−0.31	−22.44	6.53	–	–	–
	Summer	−0.28	−12.12	3.69	−0.27	−24.09	7.67	–	–	–
	Fall	–	–	–	–	–	–	–	–	–
ENF	Winter	**0.23**	**6.17**	2.18	–	–	–	–	–	–
	Spring	−0.21	−9.21	2.04	−0.21	−15.90	3.45	−0.20	−10.41	2.31
	Summer	–	–	–	−0.38	−30.64	3.14	−0.43	−31.43	2.91
	Fall	**0.17**	**6.58**	1.80	**0.23**	**14.72**	2.93	**0.18**	**10.00**	2.62
GRA	Winter	–	–	–	–	–	–	–	–	–
	Spring	−0.26	−12.71	3.39	−0.26	−27.53	7.32	−0.22	−13.81	4.42
	Summer	−0.44	−22.24	3.18	−0.61	−59.62	6.17	−0.55	−44.04	5.00
	Fall	–	–	–	–	–	–	–	–	–
MF	Winter	–	–	–	−0.79	−45.39	20.42	–	–	–
	Spring	−0.36	−15.17	4.81	−0.40	−28.20	7.97	−0.40	−15.20	4.39
	Summer	–	–	–	−0.28	−20.25	6.84	−0.48	−27.84	5.55
	Fall	–	–	–	–	–	–	–	–	–
OSH	Winter	–	–	–	–	–	–	–	–	–
	Spring	–	–	–	–	–	–	–	–	–
	Summer	–	–	–	−0.58	−32.64	6.52	−0.63	−36.43	6.72
	Fall	–	–	–	–	–	–	–	–	–
SAV	Winter	–	–	–	–	–	–	–	–	–
	Spring	–	–	–	–	–	–	–	–	–
	Summer	–	–	–	−0.86	−24.52	8.90	−0.78	−11.69	4.76
	Fall	–	–	–	−0.54	−18.99	8.37	–	–	–
WET	Winter	–	–	–	–	–	–	–	–	–
	Spring	–	–	–	**0.57**	**14.62**	6.32	**0.58**	**8.35**	3.52
	Summer	–	–	–	−0.33	−19.24	7.17	−0.30	−11.36	4.69
	Fall	–	–	–	–	–	–	–	–	–
WSA	Winter	–	–	–	−0.29	−8.04	3.44	−0.41	−8.66	2.67
	Spring	−0.29	−9.26	4.06	−0.42	−25.47	7.72	−0.44	−17.79	5.26
	Summer	–	–	–	−0.48	−33.87	9.50	−0.59	−28.52	6.43
	Fall	–	–	–	−0.60	−33.83	7.90	−0.64	−26.03	5.71

Relative (dF_{norm} in $\sigma_{flux} -1\sigma_{EF}^{-1}$) and flux sensitivity ($dF$ in g C m^{-2} month^{-1} $-1\sigma_{EF}^{-1}$) for each carbon flux with error, the flux sensitivity SE (g C m^{-2} month^{-1} $-1\sigma_{EF}^{-1}$) based on combining uncertainty both in dF_{norm} and the pooled SD of the unnormalized carbon flux (see text), are given. Bold entries indicate an increase in flux. Dashed entry is nonsignificant result (= 0) using $q = 0.05$. Note that $dF_{norm}^2 = r^2$. Bold signifies a positive value.

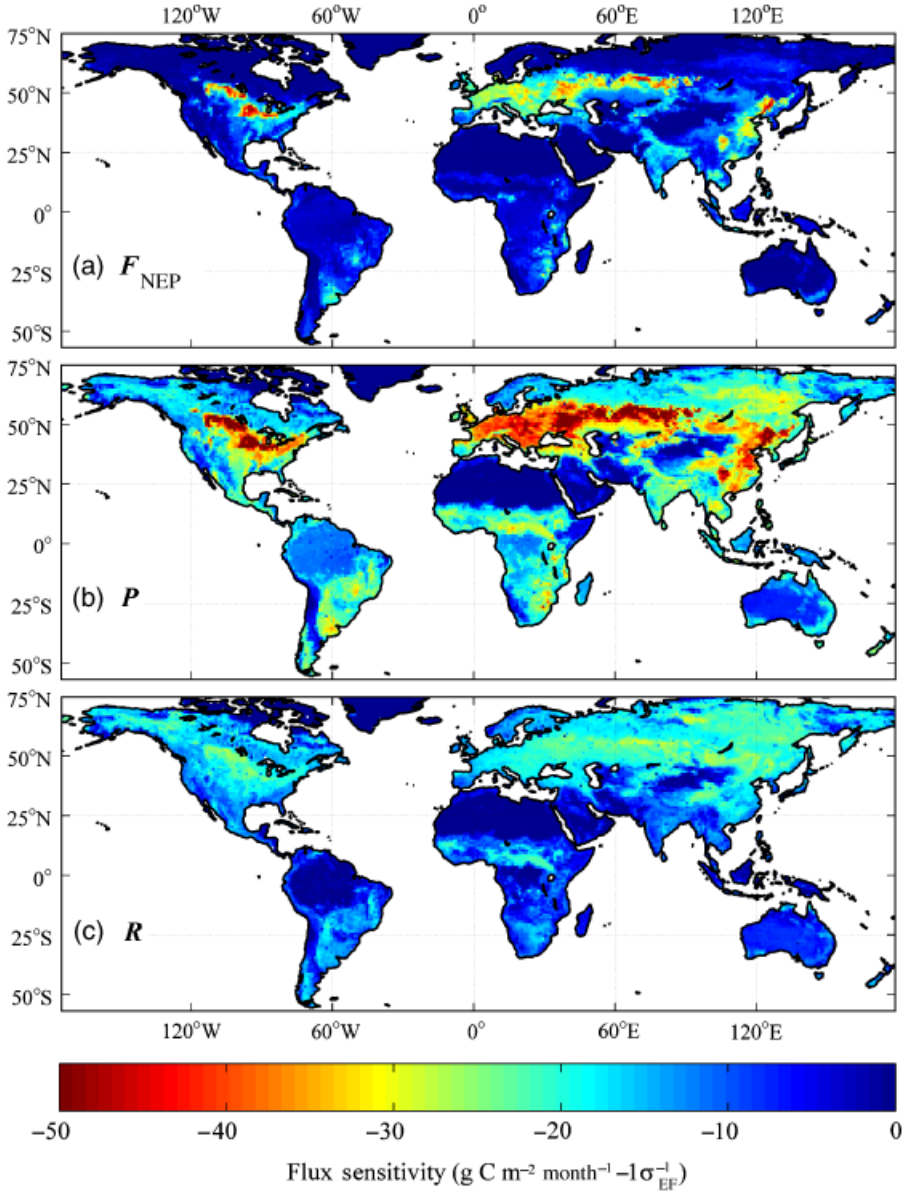

Fig. 5 Global 1° grid of mean monthly flux sensitivities to relative drought (g C m^{-2} $month^{-1}$ $-1\sigma_{EF}^{-1}$) for F_{NEP} (A), P (B), and R (C). Flux sensitivities were spatially upscaled using biome area-weighting within grid cell and averaged across climatic season using FPAR normals.

Discussion

Patterns between EF and carbon cycling

At the scales emphasized here changes in P controlled system response to relative drought. However, the exact nature of this biophysical response was based on the interplay between environmental controls represented by the EF drought metric and carbon flux responses as aggregated across space and time. As a consequence results here will not *a priori* agree with site-specific results. Despite this the analytical framework used provided for a systematic quantification of functional response to relative drought using biome–climatic season–flux data groups. This allows for data-driven comparisons between land surface model behavior and functional response as measured at FLUXNET sites (Friend *et al*., 2007) as well as the upscaling of drought sensitivities to aggregated spatial domains (Bonan, 2008). Furthermore, scaling exercises are simplified due to the linearity of carbon flux $\sim$ EF relationships in normalized space. Carbon dynamics at all levels of relative drought were additive, i.e. the response in relative carbon flux to a unit σ change in normalized

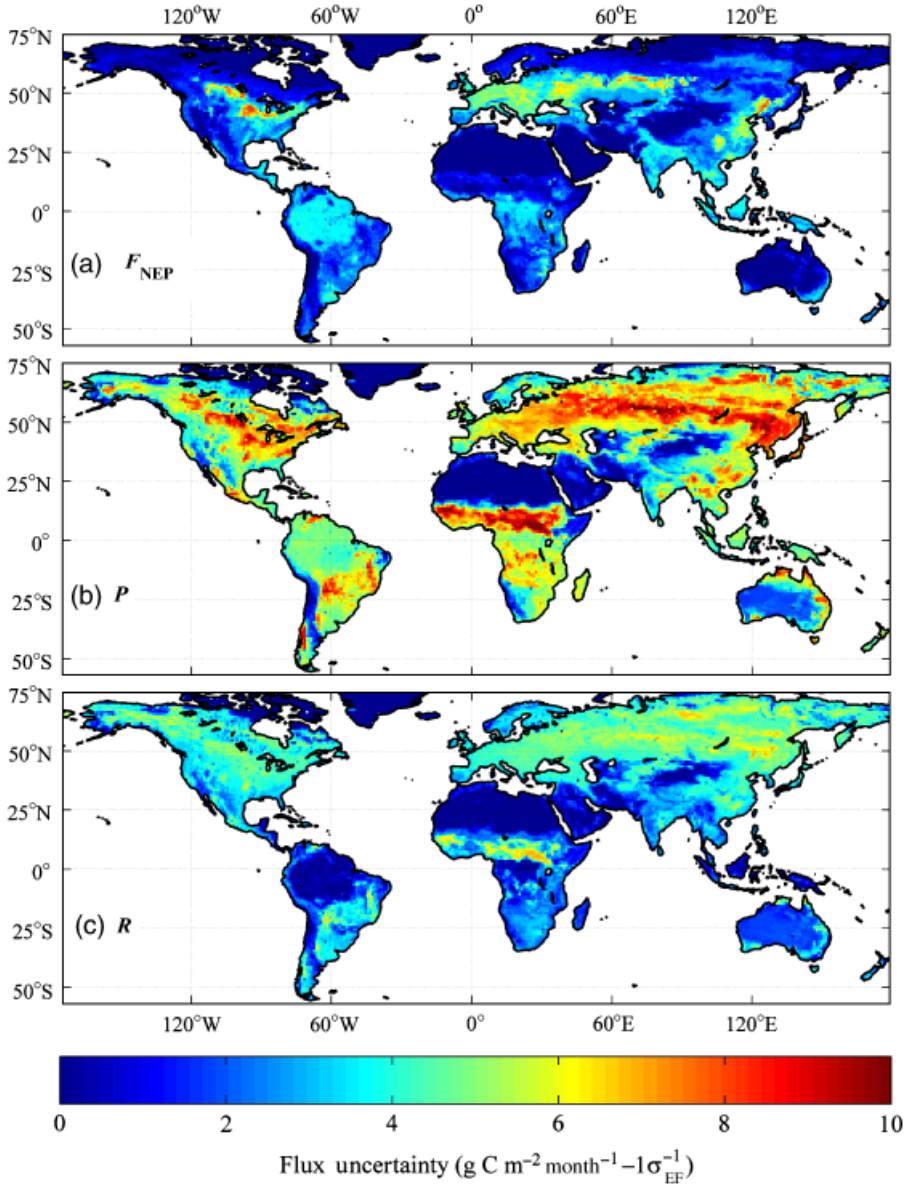

Fig. 6 Global 1° grid of mean monthly flux uncertainty to relative drought (g C m^{-2} month^{-1}–1σ_{EF}^{-1}) for F_{NEP} (A), P (B), and R (C). Uncertainties were spatially upscaled using biome area-weighting within grid cell and averaged across climatic season using FPAR normals. Note inverted color scale to match magnitude of gridded mean monthly flux sensitivities.

EF was the same in magnitude at all levels of normalized carbon flux and EF. Nonlinearities, e.g. saturation, in response to relative drought did not occur in the tails ($\approx 2\sigma$) of the distribution of normalized EF.

Spatial patterns in drought response

Spatial patterns (Fig. 5) were driven by the clustering and relative proportion of highly sensitive biomes, primarily CRO (Table 2). Agricultural systems are intensively managed and feature cultivars selected genetically for accelerated growth and enhanced yield. This suggests that CRO are less acclimated to adverse growing conditions, e.g. heat and water stress (Gervois *et al*., 2004; Barnabás *et al*., 2008; Battisti & Naylor, 2009), than more natural systems and consequently more at risk to drought effects. This is underscored by the increased use of agronomic treatments, i.e. more realistic crop parameterizations, of CRO in land surface models (e.g. de Noblet-Ducoudré *et al*., 2004) that go beyond modeling carbon flux dynamics in agricultural systems using GRA as a proxy (Bondeau *et al*., 2007). Furthermore, the drought sensitivity of croplands reinforces concerns over food production, yield safety,

and food security under forecasted climate change (Barnabás *et al*., 2008; Battisti & Naylor, 2009). In contrast, agricultural systems exhibit a large variability in management regime, e.g. intercropping, tillage, irrigation, fertilization, winter cover (Hutchinson *et al*., 2007; Furon *et al*., 2008), which translated into higher uncertainty (Table 2) and a wider range of normalized EF and carbon flux. While 29 CRO sites were analyzed, insufficient ancillary information and replication precluded disambiguating these potentially confounding effects, including site-specific treatment of carbon removal (Li *et al*., 2005).

Drought-induced increases in carbon flux

In seven biome–climatic season–flux groups drought acted to increase carbon flux. In EBF climatic winter, the onset of the tropical dry season (most EBF sites were tropical and located in Brazil), F_{NEP} exhibited a positive sensitivity to normalized EF (Table 2), i.e. became more positive during episodes of relative drought. This suggested that dry season λE was decoupled from precipitation and vegetation had access to deep water stores (Hutyra *et al*., 2007; Saleska *et al*., 2007; Bonal *et al*., 2008). Furthermore, Amazonia is a radiation-limited environment (Nemani *et al*., 2003; Teuling *et al*., 2009) with relatively drier conditions linked to decreased cloudiness, higher insolation, and greater carbon uptake (Huete *et al*., 2006; Hutyra *et al*., 2007; Saleska *et al*., 2007; Bonal *et al*., 2008). In contrast, peak rates of carbon sequestration occur at light levels less than the clear sky condition (Gu *et al*., 1999) and are generally greater under diffuse light conditions (Knohl & Baldocchi, 2008). At this aggregated spatial scale it was impossible to resolve which mechanism controlled drought response in tropical EBF systems. However, simulation studies suggest that both mechanisms operate simultaneously (Baker *et al*., 2008).

In ENF all three carbon fluxes showed positive sensitivities in climatic fall, i.e. increased under relative drought. In climatic winter F_{NEP} was also enhanced by relative drought (Table 2). Carbon cycling in ENF is related to temperature gradients (Law *et al*., 2002; Reichstein *et al*., 2007b; Baldocchi 2008), especially in northern temperate and boreal regions (Nemani *et al*., 2003) where 50 of 67 ENF sites were located. Negative relative anomalies in EF indicated warmer temperature trends ($P<0.0001$; $r=-0.18$). As EF decreased, H and both canopy and air temperature increased which in turn led to an increase in all three carbon fluxes, especially P.

Lastly, WET showed a positive response to relative drought in climatic spring for P and R (Table 2). In these systems hydrology, i.e. EF, particularly λE, is driven by water table depth (WTD) with soil moisture content a function of topography and subsurface flow (Lindroth *et al*., 2007; Baldocchi, 2008; Sonnentag *et al*., 2008). However, the robustness of this linkage remains ambiguous. Lindroth *et al*. (2007), in their analysis of four Scandinavian mires, showed that P and R were strongly dependent on WTD. In contrast, Laeur *et al*. (2005) analyzed an ombrotrophic bog located near Ottawa, Canada and found that WTD was not a significant control for R. Finally, during a drought episode at a boreal sedge fen in southern Finland carbon uptake declined with WTD being one of many relevant environmental controls (Aurela *et al*., 2007). This lack of coherent functional response may be further confounded by spatiotemporal resolution (Lindroth *et al*., 2007), within-biome variation (Aurela *et al*., 2007), and sampling frame; only four WET sites (three in Fenno-Scandinavia, one in Poland) were available in climatic spring. We hypothesize that, at the biome level, relative drought in climatic spring moved the WTD closer to its optimal level (Moore & Dalva, 1993). A relative drying increased the extent of the active unsaturated substrate layer (Limpens *et al*., 2008) and lowered the degree of spring inundation (Kurbatova *et al*., 2002); in turn this drawdown in WTD led to an increase in both gross fluxes.

Available energy and phenology

The response of DBF sites to normalized EF during climatic spring was among the largest observed (Table 2) but was an instance where EF was not solely linked to relative drought. Plant available water in climatic spring typically increases as a result of spring recharge; this and the concomitant onset of the warm season favor the partitioning of available energy toward λE and act to increase EF (Schwartz & Chen, 2002; Kim & Wang, 2005). The emergence of new foliage in deciduous systems decreases albedo and influences the partitioning of available energy (Hogg *et al*., 2000; Schwartz & Chen, 2002; Barr *et al*., 2004; Bonan, 2008). In this context, negative relative anomalies in EF corresponded to a shorter growing season length, i.e. a relative lack of λE (and smaller EF) indicated an absence of foliage and therefore fewer days of carbon uptake. However, this correlation with EF as an index of moisture status was not prognosticative. Rather, positive EF anomalies in springtime resulted from the interplay of seasonal phenological cues (e.g. photoperiod) and processes with longer-term memory (e.g. growing degree days).

The drought metric

Drought is a reoccurring phenomenon in all biomes and climates (Larcher, 1995) and occurs when plant uptake

of water is restricted and this restriction leads to an impairment of plant function. Generally, turgor in guard cells decreases, stomata close and both assimilation and transpiration are curtailed. Respiration, particularly the soil component, is also impacted through changes in soil biological life and soil aeration as mediated by soil moisture status (Verstraeten *et al*., 2006).

While EF as a drought metric had a clear biophysical interpretation and linked directly to site water status, there were instances where EF expressed a radiation or temperature response, albeit related to a drought-induced change in ecosystem state. However, for DBF in climatic spring EF tracked leaf onset as opposed to drought. Furthermore, long-term data from ecosystems sensitive to precipitation/temperature changes suggest that transient responses of vegetation may be difficult to predict due to lags and positive feedbacks (Camill & Clark, 2000). This highlights shortcomings concerning ecosystem memory, e.g. high litterfall in a drought year, leading to higher heterotrophic respiration in subsequent years (Arnone *et al*., 2008). Such processes are not well represented by relations between short-term carbon fluxes and EF as implemented in this study.

An additional caveat related to the sources of uncertainty for flux sensitivities. The largest uncertainties by biome were observed in MF and CRO. In both instances this uncertainty was confounded by non-drought factors, within-biome variability in vegetative cover and management regime, respectively. Mixed forests are comprised of interspersed mosaics of the four other forested biomes (Table 1). This adds to within-biome variability, inflates uncertainty, and increases the effective sample size needed to estimate statistically robust sensitivities. Croplands exhibit a wide range of management regime that, as a confounding factor, similarly inflates uncertainty but is not linked to drought *per se*. In both cases further stratification of FLUXNET data by climate (and management regime for CRO) is desirable but was not undertaken due to sample size limitations (Table 1).

Representativeness of FLUXNET

Finally, the sparseness of the global sampling framework influenced the robustness of carbon flux $\sim$ EF relationships. Although the compilation used in this study consisted of EC data from 238 towers extending from calendar years 1991–2006 numerous combinations of biome and climatic season were poorly sampled (Table 2), 21 of 44 possible biome–climatic season combinations having $\leq$ 10 sites. To achieve a more nuanced process-based understanding and statistically more robust estimate of carbon flux sensitivity, the coverage of FLUXNET needs to be increased toward undersampled biomes (e.g. shrublands, savannahs, and wetlands), highly variable biomes (croplands), biomes with high degrees of uncertainty (mixed forest and croplands), and underrepresented areas in general [Africa and vast tracts of Asia (Sundareshwar *et al*., 2007); Fig. 1]. The use of PFTs (biome or biome–climatic season groups) is also problematic. PFTs are vehicles of simplification, particularly in modeling where their use reduces parameter space. However, sites within a given PFT still exhibit a wide range of variability relative to climatic drivers and ecosystem state variables (Purves & Pacala, 2008), confounding estimation of EF sensitivities. Furthermore, an ANOVA model using biome, carbon flux, and climatic season as factors explained $\approx$ 60% of the variation in carbon flux response to relative drought. Taken together these points underscore the importance of additional measurement fields and sampling points to quantify other potential axes of variation in flux response to relative drought such as ecosystem state variables, edaphic properties, climatic classification (climate regime at EC tower installations is skewed toward temperate and subtropical climates), management regime (especially in intensively managed agricultural systems), and exogenous variables [e.g. nitrogen deposition (Magnani *et al*., 2007)].

Conclusion

Combining micrometeorological measurements from 238 EC towers across 11 biomes with EF as a drought metric provided a framework to systematically quantify carbon flux response to drought events. Ecosystem response to relative drought, expressed in relative or flux sensitivity, across biome, climatic season, and 1° grid cells, was driven by *P*. Overall the sensitivity of *P* to relative drought was 50% larger in magnitude than that of *R* and drought events induced a net decline in the terrestrial sink. Spatial patterns of carbon flux response to relative drought were linked to the distribution of intensively managed agricultural systems, particularly in China, Eurasia, and North America. Croplands exhibited the largest drought-induced decline in net and gross ecosystem productivity; highlighting concerns about food security under forecasted climate change. Weaknesses of this method related to an emphasis on shorter-term dynamics, DBF in climatic spring where carbon flux response was largely driven by phenology, and sensitivities for MF and CRO that were confounded by nondrought effects. A major advantage of this method was the use of relative anomalies to analyze drought episodes. This rescaling removed spatial gradients and ensured that each site contributed data points indicative of drought episodes. An additional strength related to

the linearity of response and concomitant ease of upscaling. Furthermore, EF as a drought metric yielded a well-defined biophysical interpretation, tracked historical drought episodes, and obviated the need for poorly sampled edaphic variables. Finally, synthesizing across FLUXNET allowed a global flux perspective through the integration of site-specific relationships while providing a data-driven quantification of drought response at more aggregated scales and simultaneously highlighting where additional EC installations are desirable.

Acknowledgements

C. R. S., C. A. W., and K. S. were supported by the US National Science Foundation under grant ATM-0910766. We thank the FLUXNET site PIs for contributing data, and the agencies and institutions that funded long-term measurements at these sites. This project resulted from the 2007 La Thuile FLUXNET workshop, with financial support provided by CarboEuropeIP, FAO-GTOS-TCO, iLEAPS, Max Planck Institute for Biogeochemistry, National Science Foundation, University of Tuscia, US Department of Energy (Terrestrial Carbon program; #DE-FG02-04ER63911). Moreover, we acknowledge databasing and technical support from Berkeley Water Center, Lawrence Berkeley National Laboratory, Microsoft Research eScience, Oak Ridge National Laboratory, University of California – Berkeley, University of Virginia. The following networks participated with flux data: AmeriFlux, AfriFlux, AsiaFlux, CarboAfrica, CarboEuropeIP, ChinaFlux, Fluxnet-Canada, KoFlux, LBA, NECC, OzFlux, TCOS Siberia, USCCC.

References

Akaike H (1974) A new look at the statistical model identification. *IEEE Transactions on Automatic Control*, **19**, 716–723.

Arnone JA, Verburg PSJ, Johnson DW *et al*. (2008) Prolonged suppression of ecosystem carbon dioxide uptake after an anomalously warm year. *Nature*, **455**, 383–386.

Aurela M, Riutta T, Laurila T *et al*. (2007) CO_2 balance of a sedge fen in southern Finland: the impact of drought period. *Tellus B*, **59**, 826–837.

Baker IT, Prihodko L, Denning AS, Goulden M, Miller S, da Rocha HR (2008) Seasonal drought stress in the Amazon: reconciling models and observations. *Journal of Geophysical Research*, **113**, G00B01, doi: 10.1029/2007JG000644.

Baldocchi D (2008) Breathing of the terrestrial biosphere: lessons learned from a global network of carbon dioxide ux measurement systems. *Australian Journal of Botany*, **56**, 1–26.

Baldocchi D, Falge E, Gu LH *et al*. (2001) FLUXNET: a new tool to study the temporal and spatial variability of ecosystem-scale carbon dioxide, water vapor, and energy flux densities. *Bulletin of the American Meteorological Society*, **82**, 2415–2434.

Barnabás B, Jäger K, Fehér A (2008) The effect of drought and heat stress on reproductive success in cereals. *Plant, Cell, and Environment*, **31**, 11–38.

Barr AG, Black TA, Hogg EH *et al*. (2007) Climatic controls on the carbon and water balances of a boreal aspen forest, 1994–2003. *Global Change Biology*, **13**, 561–576.

Barr AG, Black TA, Hogg EH, Kljun N, Morgenstern K, Nesic Z (2004) Inter-annual variability in the leaf area index of a boreal aspen-hazelnut forest in relation to net ecosystem production. *Agricultural and Forest Meteorology*, **126**, 237–255.

Battisti DS, Naylor RL (2009) Historical warnings of future food insecurity with unprecedented seasonal heat. *Science*, **323**, 240–244.

Belward A, Loveland T (1996) *The DIS 1 km land cover data set*. Global Change, The IGBP Newsletter, 27.

Benjamini Y, Hochberg Y (1995) Controlling the false discovery rate: a practical and powerful approach to multiple testing. *Journal of the Royal Statistical Society, Series B*, **57**, 289–300.

Bonal D, Bosc A, Goret JY *et al*. (2008) The impact of severe dry season on net ecosystem exchange in the neotropical rainforest of French Guiana. *Global Change Biology*, **14**, 1917–1933.

Bonan GB (2008) Forests and climate change: forcings, feedbacks, and the climate benefits of forests. *Science*, **320**, 1444–1445.

Bondeau A, Smith PC, Zaehle S *et al*. (2007) Modelling the role of agriculture for the 20th century global terrestrial carbon balance. *Global Change Biology*, **13**, 679–706.

Brutsaert WH (1982) *Evaporation into the Atmosphere: Theory, History, and Applications*. D. Reidel Publishing Co., Dordrecht.

Camill P, Clark JS (2000) Long-term perspectives on lagged ecosystem responses to climate change: permafrost in boreal peatlands and the grassland/woodland boundary. *Ecosystems*, **3**, 534–544.

Canadell JG, Le Quéré C, Raupach MR *et al*. (2007) *Contributions to accelerating atmospheric CO_2 growth from economic activity, carbon intensity, and efficiency of natural sinks*. Proceedings of the National Academy of Science, 0702737104.

Ciais P, Reichstein M, Viovy N *et al*. (2005) Europe-wide reduction in primary productivity caused by the heat and drought in 2003. *Nature*, **437**, 529–533.

Cook ER, Woodhouse CA, Eakin CM, Meko DM, Stahle DW (2004) Long-term aridity changes in the western United States. *Science*, **306**, 1015–1018.

Dai A, Lamb PJ, Trenberth KE, Hulme M, Jones PD, Pingping X (2004a) The recent Sahel drought is real. *International Journal of Climatology*, **24**, 1323–1331.

Dai A, Trenberth KE, Qian T (2004b) A global data set of Palmer Drought Severity Index for 1870–2002: relationship with soil moisture and effects of surface warming. *Journal of Hydrometeorology*, **5**, 1117–1130.

de Noblet-Ducoudré N, Gervois S, Ciais P *et al*. (2004) Coupling the soil–vegetation–atmosphere-transfer scheme ORCHIDEE to the agronomy model STICS to study the influence of croplands on the European carbon and water budgets. *Agronomie*, **24**, 1–11.

Efron B, Tibshirani RJ (1998) *An Introduction to the Bootstrap*. Chapman & Hall/CRC, Boca Raton.

Foken T (2008) The energy balance closure problem – an overview. *Ecology and Application*, **18**, 1351–1367.

Friend AD, Arneth A, Kiang NY *et al*. (2007) FLUXNET and modelling the global carbon cycle. *Global Change Biology*, **13**, 610–633.

Furon AC, Wagner-Riddle C, Smith CR, Warland JS (2008) Wavelet analysis of wintertime and spring thaw CO_2 and N_2O fluxes from agricultural fields. *Agricultural and Forest Meteorology*, **148**, 1305–1317.

Gervois S, de Noblet-Ducoudré N, Viovy N *et al*. (2004) Including croplands in a global biosphere model: methodology and evaluation at specific sites. *Earth Interactions*, **8**, 1–25.

Granier A, Reichstein M, Breda N *et al*. (2007) Evidence for soil water control on carbon and water dynamics in European forests during the extremely dry year: 2003. *Agricultural and Forest Meteorology*, **143**, 123–145.

Groisman PY, Sherstyukovb BG, Razuvaev VN *et al*. (2007) Potential forest re danger over northern Eurasia: changes during the 20th century. *Global and Planetary Change*, **56**, 371–386.

Gu L, Fuentes JD, Shugart HH, Staebler RM, Black TA (1999) Responses of net ecosystem exchanges of carbon dioxide to changes in cloudiness: results from two North American deciduous forests. *Journal of Geophysical Research*, **104**, 31421–31434.

Hastie T, Tibshirani R, Friedman J (2003) *The Elements of Statistical Learning*. Springer Verlag, New York.

Heim RR (2002) A review of twentieth-century drought indices used in the United States. *Bulletin of the American Meteorological Society*, **83**, 1149–1165.

Hogg EH, Price DT, Black TA (2000) Postulated feedbacks of deciduous forest phenology on seasonal climate patterns in the Western Canadian interior. *Journal of Climatology*, **13**, 4229–4243.

Hollinger DY, Richardson AD (2005) Uncertainty in eddy covariance measurements and its application to physiological models. *Tree Physiology*, **25**, 873–885.

Houghton RA (2000) Interannual variability in the global carbon cycle. *Journal of Geophysical Research*, **105** (D15), 20,121–20,130.

Houghton RA (2007) Balancing the global carbon budget. *Annual Review of Earth and Planetary Sciences*, **35**, 313–347.

Huete AR, Didan K, Shimabukuro YE *et al*. (2006) Amazon rainforests green-up with sunlight in dry season. *Geophysical Research Letters*, **33**, L06405, doi: 10.1029/2005GL025583.

Huntington TG (2006) Evidence for intensication of the global water cycle: review and synthesis. *Journal of Hydrology*, **319**, 83–95.

Hutchinson JJ, Campbell CA, Desjardins RL (2007) Some perspectives of carbon sequestration in agriculture. *Agricultural and Forest Meteorology*, **142**, 288–302.

Hutyra LR, Munger JW, Saleska SR *et al*. (2007) Seasonal controls on the exchange of carbon and water in an Amazonian rain forest. *Journal of Geophysical Research*, **112**, G03008, doi: 10.1029/2006JG000365.

Kim Y, Wang G (2005) Modeling seasonal vegetation variation and its validation against Moderate Resolution Imaging Spectroradiometer (MODIS) observations over North America. *Journal of Geophysical Research*, **110**, D04106, doi: 10.1029/2004JD005436.

Kljun N, Black TA, Griffis TJ *et al*. (2007) Response of net ecosystem productivity of three boreal forest stands to drought. *Ecosystems*, **10**, 1039–1055.

Knohl A, Baldocchi DD (2008) Effects of diffuse radiation on canopy gas exchange processes in a forest ecosystem. *Journal of Geophysical Research*, **113**, G02023, doi: 10.1029/2007JG000663.

Kurbatova J, Arneth A, Vygodskaya NN *et al*. (2002) Comparative ecosystem–atmosphere exchange of energy and mass in a European Russian and a central Siberian bog I. Interseasonal and interannual variability of energy and latent heat fluxes during the snowfree period. *Tellus B*, **54**, 497–513.

Kurc SA, Small EE (2004) Dynamics of evapotranspiration in semiarid grassland and shrubland ecosystems during the summer monsoon season, central New Mexico. *Water Resources and Research*, **40**, W09305, doi: 10.1029/2004WR003068.

Laeur PM, Moore TR, Roulet NT, Frolking S (2005) Ecosystem respiration in a cool temperate bog depends on peat temperature but not water table. *Ecosystems*, **8**, 619–629.

Larcher W (1995) *Physiological Plant Ecology*. Springer Verlag, Berlin.

Lauenroth WK, Sala OE (1992) Long-term forage production of North American shortgrass steppe. *Ecological Applications*, **4**, 397–403.

Law BE, Falge E, Baldocchi DD *et al*. (2002) Environmental controls over carbon dioxide and water vapor exchange of terrestrial vegetation. *Agricultural and Forest Meteorology*, **113**, 97–120.

Law BE, Goldstein AH, Anthoni PM *et al*. (2001) Carbon dioxide and water vapor exchange by young and old ponderosa pine ecosystems during a dry summer. *Tree Physiology*, **21**, 299–308.

Li SG, Asanuma J, Eugster W *et al*. (2005) Net ecosystem carbon dioxide exchange over grazed steppe in central Mongolia. *Global Change Biology*, **11**, 1941–1955.

Limpens J, Berendse F, Blodau C *et al*. (2008) Peatlands and the carbon cycle: from local processes to global implications – a synthesis. *Biogeosciences*, **5**, 1475–1491.

Lindroth A, Lagergren F, Grelle A, Klemedtsson L, Langval O, Weslien P, Tuulik J (2009) Storms can cause Europe-wide reduction in forest carbon sink. *Global Change Biology*, **15**, 346–355.

Lindroth A, Lund M, Nilsson M *et al*. (2007) Environmental controls on the CO_2 exchange in north European mires. *Tellus B*, **59**, 812–826.

Lo E (2005) Gaussian error propagation applied to ecological data: post-ice-storm-downed woody biomass. *Ecological Monographs*, **75**, 451–466.

Loveland TR, Reed BC, Brown JF, Ohlen DO, Zhu J, Yang L, Merchant JW (2001) Development of a global land cover characteristics database and IGBP DISCover from 1-km AVHRR data. *International Journal of Remote Sensing*, **21**, 1303–1330.

Magnani F, Mencuccini M, Borghetta M *et al*. (2007) The human footprint in the carbon cycle of temperate and boreal forests. *Nature*, **447**, 848–850.

Marengo JA, Nobre CA, Tomasella J *et al*. (2008) The drought of Amazonia in 2005. *Journal of Climatology*, **21**, 495–516.

McQuarrie ADR, Tsai CL (1998) *Regression and Time Series Model Selection*. World Scientific, Singapore.

Moffat A, Papale D, Reichstein M *et al*. (2007) Comprehensive comparison of gap-filling techniques for eddy covariance net carbon fluxes. *Agricultural and Forest Meteorology*, **147**, 209–232.

Moore TR, Dalva M (1993) The influence of temperature and water table position on carbon dioxide and methane emissions from laboratory columns of peatland soils. *European Journal of Soil Science*, **44**, 651–664.

Mu QF, Heinsch FA, Zhao M, Running SW (2007) Development of a global evapotranspiration algorithm based on MODIS and global meteorology data. *Remote Sensing of Environment*, **111**, 519–536.

Nemani RR, Keeling CD, Hashimoto H *et al*. (2003) Climate-driven increases in global terrestrial net primary production from 1982 to 1999. *Science*, **300**, 1560–1563.

Nicholls N (2004) The changing nature of Australian droughts. *Climatic Change*, **63**, 323–336.

Papale D, Reichstein M, Aubinet M *et al*. (2006) Towards a standardized processing of net ecosystem exchange measured with eddy covariance technique: algorithms and uncertainty estimation. *Biogeosciences*, **3**, 571–583.

Papale D, Valentini R (2003) A new assessment of European forests carbon exchanges by eddy fluxes and artificial neural network spatialization. *Global Change Biology*, **9**, 525–535.

Pereira JS, Mateus JA, Aires LM *et al*. (2007) Net ecosystem carbon exchange in three contrasting Mediterranean ecosystems – the effect of drought. *Biogeosciences*, **4**, 791–802.

Purves DW, Pacala S (2008) Predictive models of forest dynamics. *Science*, **320**, 1452–1453.

Reichstein M, Ciais P, Papale D *et al*. (2007a) Reduction of ecosystem productivity and respiration during the European summer 2003 climate anomaly: a joint flux tower, remote sensing and modelling analysis. *Global Change Biology*, **13**, 634–651.

Reichstein M, Falge E, Baldocchi DD *et al*. (2005) On the separation of net ecosystem exchange into assimilation and ecosystem respiration: review and improved algorithm. *Global Change Biology*, **11**, 1424–1439.

Reichstein M, Papale D, Valentini R *et al*. (2007b) Determinants of terrestrial ecosystem carbon balance inferred from European eddy covariance flux sites. *Geophysical Research Letters*, **34**, L01402, doi: 10.1029/2006GL027880.

Richardson AD, Hollinger DY, Aber JD, Ollinger SV, Braswell BH (2007) Environmental variation is directly responsible for short- but not long-term variation in forest-atmosphere carbon exchange. *Global Change Biology*, **13**, 788–803.

Richardson AD, Hollinger DY, Burba GG *et al*. (2006) A multi-site analysis of random error in tower-based measurements of carbon and energy fluxes. *Agricultural and Forest Meteorology*, **136**, 1–18.

Saleska SR, Didan K, Huete AR, da Rocha HR (2007) Amazon forests green-up during 2005 drought. *Science*, **318**, 612.

San Miguel-Ayanz J, Vogt J, De Roo A, Schmuck G (2000) Natural hazards monitoring: forest fires, droughts and floods – the example of European pilot projects. *Surveys in Geophysics*, **21**, 291–305.

Schwartz MD, Chen X (2002) Examining the onset of spring in China. *Climate Research*, **21**, 157–164.

Schwarz PA, Law BE, Williams M, Irvine J, Kurpius M, Moore D (2004) Climatic versus biotic constraints on carbon and water fluxes in seasonally drought-affected ponderosa pine ecosystems. *Global Biogeochemical Cycles*, **18**, GB4007, doi: 10.1029/2004GB002234.

Shabbar A, Skinner W (2004) Summer drought patterns in Canada and the relationship to global sea surface temperatures. *Journal of Climatology*, **17**, 2866–2880.

Shao CL, Chen JQ, Li LH *et al*. (2008) Spatial variability in soil heat flux at three Inner Mongolia steppe ecosystems. *Agricultural and Forest Meteorology*, **148**, 1433–1443.

Sonnentag O, Chen JM, Roulet NT, Ju W, Govind A (2008) Spatially explicit simulation of peatland hydrology and carbon dioxide exchange: influence of mesoscale topography. *Journal of Geophysical Research*, **113**, G02005, doi: 10.1029/2007JG000605.

Sundareshwar PV, Murtugudde R, Srinivasan G *et al*. (2007) Environmental monitoring network for India. *Science*, **316**, 204–205.

Taylor JR (1996) *An Introduction to Error Analysis*. University Science Books, Mill Valley, CA, USA.

Teuling AJ, Hirschi M, Ohmura A *et al*. (2009) A regional perspective on trends in continental evaporation. *Geophysical Research Letters*, **36**, L02404, doi: 10.1029/2008GL036584.

Trenberth KE, Guillemot CJ (1996) Physical processes involved in the 1988 drought and 1993 floods in North America. *Journal of Climate*, **9**, 1288–1298.

Trenberth KE, Jones PD, Ambenje P *et al*. (2007) Observations: surface and atmospheric climate change. In: *Climate Change 2007: The Physical Science Basis. Contribution of Working Group I to the Fourth Assessment Report of the Intergovernmental Panel on Climate Change* (eds Solomon SD *et al*.), pp. 235–336. Cambridge University Press, Cambridge, UK.

Tucker CJ, Pinzon JE, Brown ME *et al*. (2005) An extended AVHRR 8-km NDVI data set compatible with MODIS and SPOT vegetation NDVI data. *International Journal of Remote Sensing*, **26**, 4485–5598.

Ventura V, Paciorek CJ, Risbey JS (2004) Controlling the proportion of falsely-rejected hypotheses when conducting multiple tests with climatological data. *Journal of Climate*, **17**, 4343–4356.

Verstraeten WW, Veroustraete F, Feyen J (2006) On temperature and water limitation of net ecosystem productivity: implementation in the C-Fix model. *Ecological Modelling*, **199**, 4–22.

Wilson KB, Goldstein A, Falge E *et al*. (2002) Energy balance closure at FLUXNET sites. *Agricultural and Forest Meteorology*, **113**, 223–243.

Zou XK, Zhai PM, Zhang Q (2005) Variations in droughts over China: 1951–2003. *Geophysical Research Letters*, **32**, L04707, doi: 10.1029/2004GL021853.